Mon. Not. R. Astron. Soc. **351,** 117–124 (2004) doi:10.1111/j.1365-2966.2004.07759.x

Taking measure of the Andromeda halo: a kinematic analysis of the giant stream surrounding M31

R. Ibata,[1★] S. Chapman,[2] A. M. N. Ferguson,[3] M. Irwin,[4] G. Lewis[5] and A. McConnachie[4]

[1]*Observatoire de Strasbourg, 11, rue de l'Université, Strasbourg F-67000, France*
[2]*California Institute of Technology, Pasadena, CA 91125, USA*
[3]*Max-Plank-Institut für Astrophysik, Karl-Schwarzschild-Str. 1, Postfach 1317, Garching D-85741, Germany*
[4]*Institute of Astronomy, Madingley Road, Cambridge CB3 0HA*
[5]*Institute of Astronomy, School of Physics, A29, University of Sydney, NSW 2006, Australia*

Accepted 2004 February 19. Received 2004 February 4; in original form 2003 October 27

ABSTRACT

We present a spectroscopic survey of the giant stellar stream found in the halo of the Andromeda galaxy. Taken with the DEIMOS multi-object spectrograph on the Keck2 telescope, these data display a narrow velocity dispersion of 11 ± 3 km s^{-1}, with a steady radial velocity gradient of 245 km s^{-1} over the 125-kpc radial extent of the stream studied so far. This implies that the Andromeda galaxy possesses a substantial dark matter halo. We fit the orbit of the stream in different galaxy potential models. In a simple model with a composite bulge, disc and halo, where the halo follows a universal profile that is compressed by the formation of the baryonic components, we find that the kinematics of the stream require a total mass inside 125 kpc of $M_{125} = 7.5^{+2.5}_{-1.3} \times 10^{11}$ M$_\odot$, or $M_{125} > 5.4 \times 10^{11}$ M$_\odot$ at the 99 per cent confidence level. This is the first galaxy in which it has been possible to measure the halo mass distribution by such direct dynamical means over such a large distance range. The resulting orbit shows that if M32 or NGC 205 is connected with the stream, they must either trail or lag the densest region of the stream by more than 100 kpc. Furthermore, according to the best-fitting orbit, the stream passes very close to M31, causing its demise as a coherent structure and producing a fan of stars that will pollute the inner halo, thereby confusing efforts to measure the properties of genuine halo populations. Our data show that several recently identified planetary nebulae, which have been proposed as evidence for the existence of a new companion of M31, are likely members of the Andromeda stream.

Key words: galaxies: individual: M31 – galaxies: kinematics and dynamics.

1 INTRODUCTION

Stellar streams represent the visible remnants of the merging process by which the haloes of galaxies are built up. By studying these streams we can attempt to unravel the formation of galactic haloes, seeing when, how and how many small galaxies arrived and were incorporated into large galaxies (Helmi & White 1999; Johnston, Sackett & Bullock 2001). Streams are also of great interest as probes of the large-scale mass distribution of the dark haloes they reside in (Johnston et al. 1999; Zhao et al. 1999; Ibata et al. 2001a). This utility stems from the fact that streams from low-mass disrupting stellar systems trace the orbit of their progenitor, giving a means to constrain the tangential motion of the stars in the stream. The stars must move along the stream and the magnitude of the tangential velocity must be such that, when the star is integrated along the orbit, it ends up with the same velocity as the stars that are currently downstream on the same orbit.

Giant stellar streams may well be common structures around galaxies (Malin & Hadley 1997; Pohlen et al. 2003). Indeed, the most conspicuous feature in the halo of the Milky Way is the giant rosette stream originating from the Sagittarius dwarf galaxy, which contains approximately half of the high-latitude ($|b| > 30°$) intermediate-age stars at distances greater than 15 kpc (Ibata et al. 2001a 2002; Majewski et al. 2003). It would appear that the Milky Way has not incorporated into the halo a more massive galaxy than the Sagittarius dwarf over the last ∼7 Gyr.

This naturally leads to the question of whether the Milky Way has unusual feeding habits. To answer this, we have undertaken a large

★E-mail: ibata@astro.u-strasbg.fr

photometric study of M31, using the wide field cameras at the Isaac Newton Telescope (INT) and the Canada–France–Hawaii Telescope (CFHT) to resolve stars over the entire disc and inner halo of that galaxy (Ibata et al. 2001b; Ferguson et al. 2002; McConnachie et al. 2003). This has given us an unprecedented panoramic view of the large-scale and small-scale structure of a disc galaxy. The analysis of this huge data set is still in progress, but it has already yielded some surprising results regarding the incidence of substructure in the halo of M31. The most prominent of these substructures is a stream-like over-density of stars near the minor axis of M31 (Ibata et al. 2001b), at first sight a facsimile of the Sagittarius stream around the Milky Way. The red giant branch (RGB) stellar density in the halo increases on average by a factor of two in the on-stream regions and is statistically significant at the 50σ level. Interestingly, this stream points toward the Andromeda satellites M32 and NGC 205, and is aligned with the outer isophotes of NGC 205, suggesting a relationship between the Andromeda stream and these two dwarf galaxies. If this interpretation is correct, the stream has to be the result of previous interactions with M31, as there is otherwise not enough time to spatially separate it from either of the two dwarf galaxies.

The proximity of M31 provides us with an opportunity to undertake a spectroscopic survey of individual stars within the stream: indeed, Andromeda offers the only extragalactic giant galaxy in which such a study can be undertaken with current instrumentation, because in more distant systems such halo substructure would be smeared into very low surface brightness features.

One useful property of the stream is that it is on a highly radial orbit. It passes very close to the centre of M31, where a comparison of the RGB tip of the stream to that of M31 itself shows them to lie at the same distance (McConnachie et al. 2003); whereas in the furthest field in which it has been detected to date, the peak of its giant branch is 0.27 mag fainter, indicating that it is 106 ± 20 kpc behind M31 (McConnachie et al. 2003). This fortuitous alignment close to the line of sight, allows us to measure directly the potential gradient over >100 kpc and hence measure the halo mass.

The layout of this paper is as follows: Section 2 presents the spectroscopic survey of the Andromeda stream, the results of which are used in Section 3 to constrain the mass of the dark matter halo of M31; finally, in Section 4 we discuss the significance of the results and present the conclusions of this study. Throughout this work, we assume a distance of 780 kpc to M31 (Stanek & Garnavich 1998) and a systemic radial velocity of -300 km s^{-1} (de Vaucouleurs et al. 1991).

2 THE ANDROMEDA HALO SURVEY

To understand the nature of the substructures detected in our panoramic halo surveys of M31, we undertook a follow-up programme to measure the kinematics of individual RGB stars with the DEIMOS spectrograph on the Keck2 10 m telescope. On 2002 September 29–30, we used the instrument in the high-resolution configuration with the 1200 l mm^{-1} grating (giving access to the spectral region 6400 to 9000 Å) to obtain high-quality spectra of 768 stars in nine fields in M31. This has given an order of magnitude improvement in statistics over previous radial velocity surveys of the M31 system Reitzel & Guhathakurta (2002). The present contribution examines data from four fields along the giant stellar stream.

RGB stars were selected for observation from our CFHT12K camera survey, which covers the region of the sky shown schematically on the left-hand panel of Fig. 1. Stars were selected by choosing point sources with I-band magnitudes in the range $20.5 < I < 22.0$ and colours $1.0 < V - I < 4.0$. Both metal-poor and metal-rich populations will be present in this selection region (see e.g. McConnachie et al. 2003). The number of target stars per 16.9×5 arcmin^2 DEIMOS field is approximately 100. The slitlet widths were milled at 0.7 arcsec to match the median seeing and the slitlet lengths were always larger than 5 arcsec, giving access to a good estimation of the local sky.

The spectroscopic images were processed and combined using the pipeline software developed by the Deep Extragalactic Evolutionary Probe (DEEP) consortium. This software debiasses, performs a flat-field, extracts, wavelength calibrates and sky subtracts the spectra. After extracting the spectra with a boxcar algorithm, the radial velocities of the stars were measured with respect to spectra of standard stars observed during the observing run. By fitting the peak of the cross-correlation function with a Gaussian, an estimate of the radial velocity accuracy was obtained for each radial velocity measurement. The accuracy of these data are astonishing for such faint stars, with typical uncertainties of 5 to 10 km s^{-1}. Finally, M31-centred radial velocities are calculated by adding 300 km s^{-1} to the heliocentric values.

In the four stream fields 184 stars were measured with radial velocity uncertainties less than 25 km s^{-1}. The right-hand panel of Fig. 1 shows the subset of 125 stars that have heliocentric velocity $v_{\rm h} < -100$ km s^{-1}, as a function of projected distance d_δ (= 780 tan η kpc) along the declination direction. For clarity, stars with $v_{\rm h} > -100$ km s^{-1}, which are primarily Galactic, have been omitted from this diagram. These four fields correspond to CFHT fields 1, 2, 4 and 8, and their locations on the sky are marked in the left-hand panel. The heliocentric distances of the fields, as measured from the magnitude of the tip of the RGB of the stream population (McConnachie et al. 2003), are displayed in the right-hand panel of Fig. 2. The outermost field lies at ($\xi = -2\overset{\circ}{.}0$, $\eta = -4\overset{\circ}{.}1$) at a heliocentric distance of 886 ± 20 kpc, that is, it extends out to 125 ± 17 kpc from the centre of M31. This is the first time that it has been possible to measure the kinematics of a stellar stream over such a huge range in galactocentric distance. An immediately striking aspect of these data is the sharp edge to the distribution at negative velocities in Fig. 1, with a velocity gradient that appears to be almost a straight line. The velocity distribution near this edge is very narrow, as demonstrated by Fig. 3, where we show the distribution of velocity offsets from the straight line in Fig. 1. We compare the data between -40 to 40 km s^{-1} in Fig. 3 to a Gaussian model using the maximum likelihood technique and find that the dispersion is 11 ± 3 km s^{-1}. The distribution appears slightly skewed to positive velocities; defining skewness to be

$$\frac{1}{N}\sum_{j=1}^{N}\left[\frac{x_j - \overline{x}}{\sigma}\right]^3$$

(see e.g. Press et al. 1992), we find that the distribution of 82 stars in Fig. 3 that have $|v| < 100$ km s^{-1} have a skewness of 0.51. For comparison, the standard deviation of the skewness of samples of 82 stars drawn from a Gaussian distribution is 0.43, so the observed sample is not significantly skewed. Some of the stars in the skewed tail may be contaminants from the halo of M31 and others may be stream stars more distant along the line of sight. The nature of these objects may become clearer when N-body simulations are fitted to the stream.

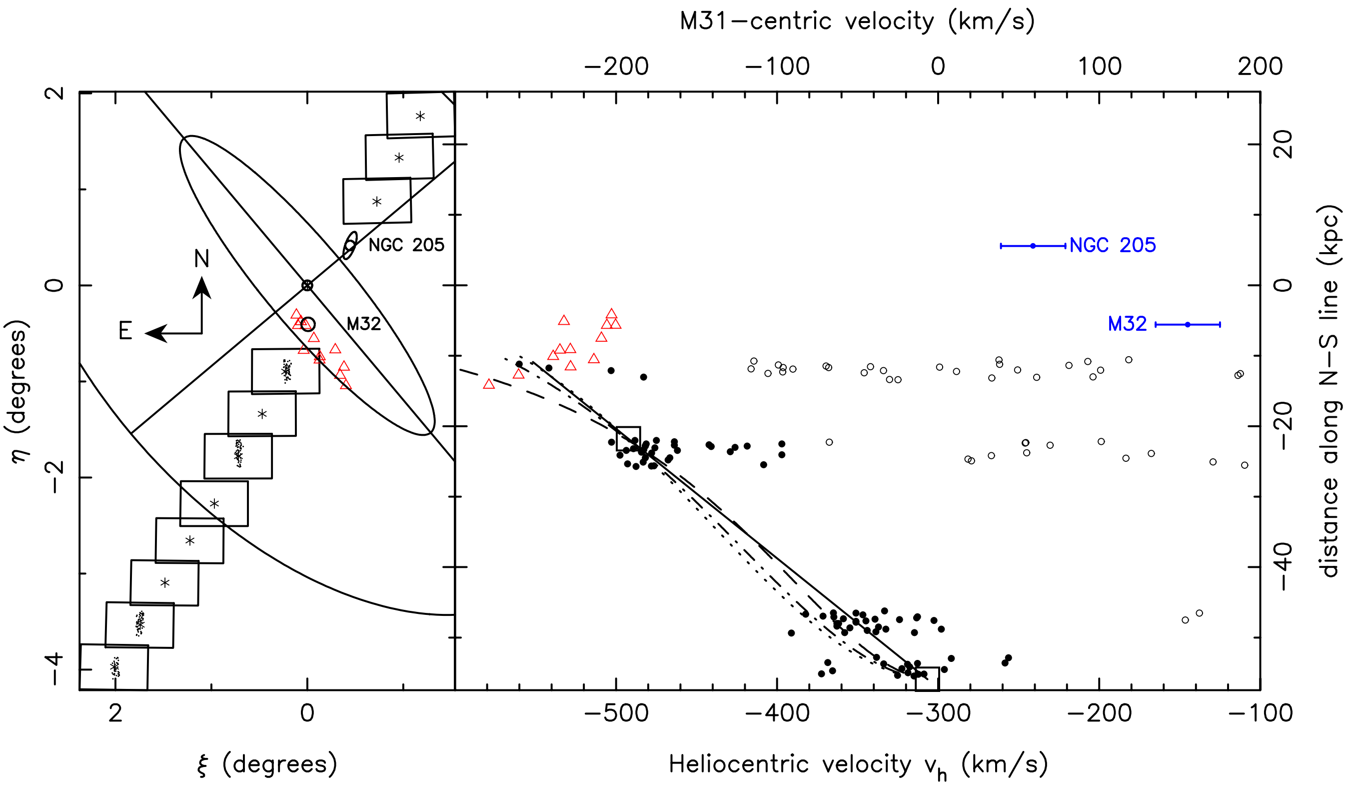

Figure 1. The left-hand panel shows the locations of the observed fields on the plane of the sky, in standard coordinates (ξ, η). Asterisk symbols denote field centres of, from south to north, fields 1–8 and 12–14 of our photometric survey of the Andromeda stream with the CFHT12K camera; while the large rectangles display the size of the CFHT12K camera pointings. The Keck2 DEIMOS targets are shown as small dots in the centre of fields 1, 2, 6 and 8. Triangles represent the positions of the planetary nebulae identified by Morrison et al. (2003). The inner ellipse demarcates the approximate limit of the visible disc of M31 at 2° (=27 kpc radius) and the outer ellipse shows a segment of a 50 kpc radius ellipse flattened to $c/a = 0.6$, corresponding to the approximate limit of our INT survey. The right-hand panel presents the radial velocity measurements (full circles), as a function of distance from M31 along the declination direction [=780 tan η kpc]. The positions of M32 and NGC 205 are also shown. The black line shows a straight-line fit [$v_h(\eta) = -4244.8 \tan \eta - 610.9$ km s^{-1}] to the high negative velocity edge of this diagram. Stars that are more than 100 km s^{-1} away from this line are marked with open circles. The two large squares show the chosen points for our back-of-the-envelope calculation, detailed in Section 3. The dashed, dot-dashed and dotted lines show the orbital paths in simple Kepler, logarithmic and NFW potentials, respectively. The velocities of the Morrison et al. (2003) planetary nebulae are represented again with triangles.

3 CONSTRAINTS ON THE DARK MATTER HALO

Before fitting an orbit model in a realistic galaxy potential through the position and velocity data, it is worth investigating what can be learned from a simple back-of-the-envelope analytic calculation. We assume that the global potential Ψ at the distance of the stream is approximated by a spherical potential and that the stream follows the orbit of the centre of mass so all stars have the same total energy $E = \Psi(r) + \frac{1}{2}\boldsymbol{v}(r)^2$, where $\boldsymbol{v}$ is the three-dimensional velocity of a star at radial position r. If we assume further that the orbit is radial, which is a reasonable approximation given the distance information in Fig. 2, then $\boldsymbol{v}(r) = v(\beta)/\cos\gamma$, where v is the observed (one-dimensional) radial velocity, as a function of angular distance

$$\beta = \cos^{-1}(\cos\xi\cos\eta) = \sin^{-1}\left(\frac{r}{780\,\mathrm{kpc}}\sin\gamma\right)$$

along the stream and γ is the projection angle on to the line of sight. The M31–Sun–field-1 triangle has an angle of $\cos^{-1}[\cos(-2\overset{\circ}{.}0)\cos(-4\overset{\circ}{.}1)]$ and lengths 780 kpc (M31–Sun), 886 ± 20 kpc (Sun–field-1) and 125 ± 17 kpc (field-1–M31). Thus the cosine of the projection angle on to the line of sight is $\cos\gamma = 0.868 \pm 0.040$. We take two data points ($\xi_1 = 2\overset{\circ}{.}0$, $\eta_1 = -4\overset{\circ}{.}1$) and ($\xi_2 = 0\overset{\circ}{.}7$, $\eta_2 = -1\overset{\circ}{.}6$), for which the de-projected Andromeda-centric distance and de-projected velocity are ($r_1 = 125 \pm 17$ kpc, $v_1 = -9 \pm 13$ km s^{-1}), ($r_2 = r_1 \sin\eta_2/\sin\eta_1 = 49 \pm 18$ kpc, $v_2 = -222 \pm 13$ km s^{-1}) to represent the stream. The uncertainty on r_1 is calculated from the projection and distance uncertainties, while the uncertainties on v_1 and v_2 are estimated from the 11 ± 3 km s^{-1} dispersion combined with the projection uncertainty. These two points correspond to the extremities of fields 1 and 6 (we do not choose field 8, as this region is much deeper in the potential, where the disc contribution is significant). In calculating these de-projected velocities, we have assumed that the tangential velocity of M31 is zero. It has long been suspected that this tangential velocity is small given that there is no other large galaxy in the Local Group to provide significant torque to the Milky Way–M31 system (Kahn & Woltjer 1959). Lynden-Bell & Lin (1977) have also pointed out that this tangential motion must be small, as there is otherwise not enough time for M31 and the Milky Way to have almost completed an orbit about each other in the age of the Universe, as is required by the Local Group timing argument. The result of Einasto & Lynden-Bell (1982) is consistent with this possibility: they find that the transverse motion of M31 is 60 ± 30 km s^{-1}, under the assumption that M31 and the Milky Way have equal and opposite angular momenta. To provide a crude assessment of the effect of the possible transverse

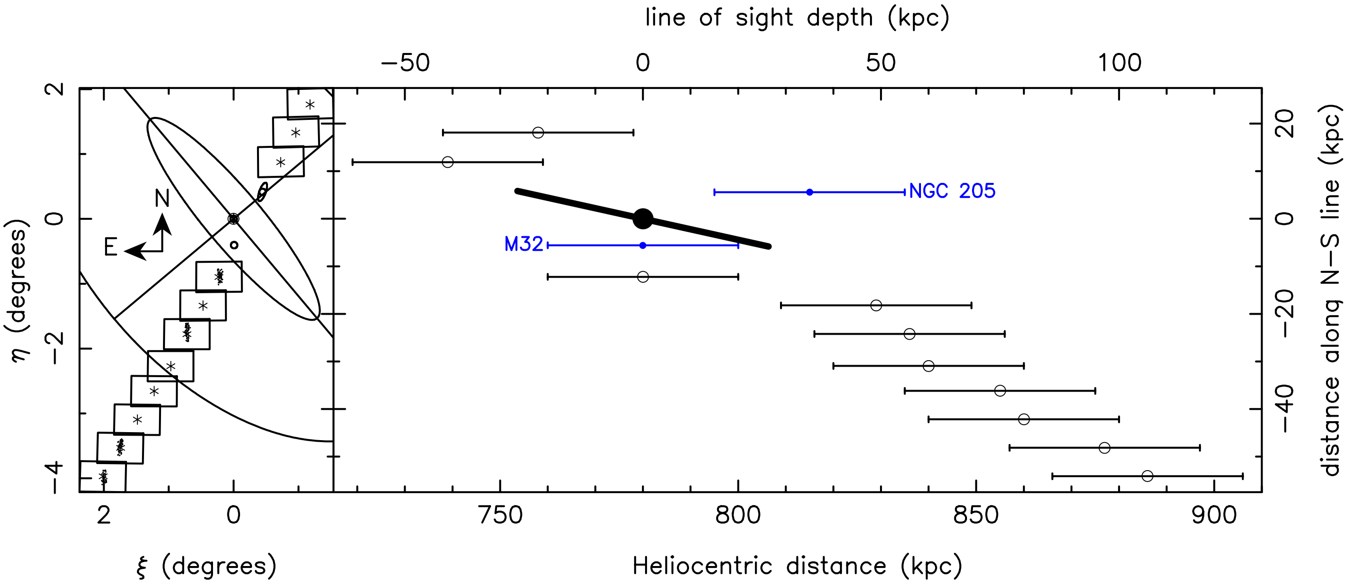

Figure 2. For convenience, the left-hand panel reproduces the chart shown previously in Fig. 1. The right-hand panel shows a sideways view of the stream, drawn to the same scale as the left-hand panel, which displays the line-of-sight depth of the fields, together with the positions of M32 and NGC 205. The disc of M31 is highly inclined to our line of sight (12°.5); the thick line is a schematic representation of a disc of radius 27 kpc inclined at 12°.5. Evidently the stream orbits close to the plane of the Andromeda galaxy.

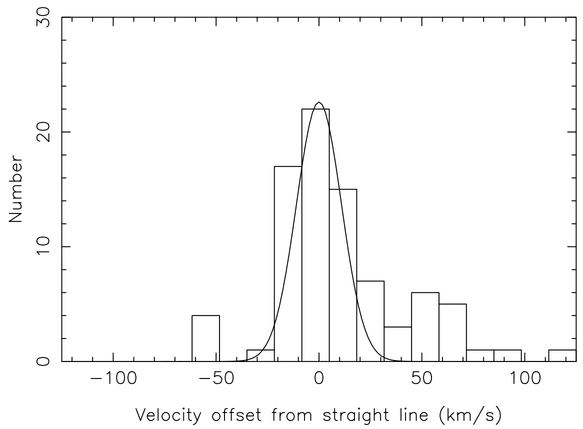

Figure 3. The distribution of velocities about the straight line displayed on the right-hand panel of Fig. 1. The stream has a narrowly-peaked velocity distribution at the position of that straight line, with dispersion 11 ± 3 km s^{-1}.

motion of M31 on the parameters derived from our data set, we also consider in the analysis below the consequence of a transverse motion of amplitude 300 km s^{-1} (i.e. equal to the radial velocity component) in the direction parallel to the stream.

For a Kepler potential, the two chosen distance and velocity data points imply a central mass of $4.6 \pm 0.7 \pm 0.3 \times 10^{11}$ $M_{\odot}$ (the second uncertainty quantifies the effect of a 300 km s^{-1} transverse velocity). A slightly more realistic case is a logarithmic potential $\Psi = \frac{1}{2} v_c^2 \log(r_c^2 + r^2)$, which has a circular velocity that asymptotes to v_c at large radius r. Following Dehnen & Binney (1998), we adopt a core radius of $r_c = 3$ kpc for this model. In this case,

$$v_c^2 = \left(v_2^2 - v_1^2\right) / \ln\left(\frac{r_c^2 + r_1^2}{r_c^2 + r_2^2}\right),$$

which gives a circular velocity of $v_c = 162 \pm 15 \pm 8$ km s^{-1}. We also investigated a simple model in which M31 is a Navarro, Frenk & White (1997, NFW) potential $\Psi = -GM_s \log\,(1 + r/r_s)\,/\,r$, where M_s is the mass within 5.3 r_s, and r_s is the scale radius. Assuming the characteristic relation between halo mass and concentration in a $z = 0$ LCDM cosmology $c = 15.0 - 3.3 \log(M_{200}/10^{12}\ M_{\odot}\ h^{-1})$ Bullock et al. (2001), we find $M_s = 4.4 \pm 1.2 \pm 0.3 \times 10^{11}$ $M_{\odot}$, ($M_{200} = 8.0 \pm 2.1 \pm 0.5 \times 10^{11}$ $M_{\odot}$, $r_{200} = 194 \pm 16 \pm 4$ kpc, $v_{200} = 136 \pm 11 \pm 3$ km s^{-1}, $r_s = 13.1 \pm 1.4 \pm 0.4$ kpc). For comparison, the mass inside 125 kpc is $7.6 \pm 1.2 \pm 0.3 \times 10^{11}$ $M_{\odot}$ for the logarithmic model and $6.4 \pm 1.3 \pm 0.3 \times 10^{11}$ $M_{\odot}$ for the NFW model, respectively. The projected distance–velocity behaviour of these three toy models is compared with the velocity measurements in Fig. 1. It is no surprise that the Keplerian potential over-predicts the radial velocity close to M31, but both the simple logarithmic and NFW halo models manage to approximate the stream velocity profile well.

To constrain more realistic models of the potential, we adopted a recent composite galaxy model by Klypin, Zhao & Somerville (2002), and calculate the potential due to a sum of disc, bulge and halo mass distributions. The bulge in this model has a mass of 1.9×10^{10} $M_{\odot}$, while the disc has a mass of 7×10^{10} $M_{\odot}$, and a scale length of 5.7 kpc. Fixing the disc and bulge with the Klypin et al. (2002) parameters (with the further assumption that the disc scale height is 400 pc, as suggested by Gould 1994), we investigate the spherical halo models compatible with our data. Following Klypin et al. (2002), we take into account the adiabatic contraction of the halo as a result of the settling of baryons into the disc and bulge, which alters the potential of the inner galaxy significantly.

We consider a halo of a given mass, with the appropriate concentration (Bullock et al. 2001), and compress the halo using the Klypin et al. (2002) relations. We then calculate the resulting potential by multipole expansion. Using an AMOEBA minimization algorithm (Press et al. 1992) we launch orbits in the potential, iteratively improving on guessed values for the initial position and velocity of a test particle on the orbit. A χ^2 goodness of fit statistic is minimized between the observed sky position, line-of-sight depth and radial velocity of the stars in our survey and the values predicted by the orbit model. This of course assumes that the stream follows the orbit of a test particle, an assumption that is reasonable if its progenitor was a relatively low-mass dwarf galaxy, which is consistent with the measured 11 ± 3 km s^{-1} velocity dispersion in the stream.

We assume that the orbit must pass through the field centres on the sky to within 0°.15 (2 kpc): this corresponds to our estimate of the uncertainty in the measurement of the location of the central peak along the stream. To constrain the distance of the stream, we take the measurements of McConnachie et al. (2003) together with their 20 kpc distance uncertainties (these uncertainties include an estimate of the systematic error in the distance measurement). The fit is also constrained with the measured radial velocities; we take all data-points within 100 km s^{-1} of the straight-line fit in Fig. 1 (those that are shown with filled circles) and adopt the fitted velocity dispersion of 11 km s^{-1} as the expected uncertainty in the velocity fit.

The relative likelihood of halo mass models can be analysed by comparing the likelihood of the orbit fit as a function of halo mass. However, we find that the result depends strongly on whether the distance data of fields 12 and 13 are included in the fit (the stream RGB population was not detected in field 14).

We first investigate the consequences of rejecting the distance data in fields 12 and 13. In those fields, McConnachie et a. (2003) may have detected the metal-rich thick disc, or a warp in the disc, instead of the actual stream itself. Without confirmation from radial velocities, we cannot be certain that the stream continues into that area of M31. Fitting only the data in fields 1 to 8, we find that the most likely model has a total mass inside 125 kpc of $M_{125} = 7.5 \times 10^{11}$ M$_\odot$; the likelihood drops by a factor of e^{-1} (i.e. 1σ) for $M_{125} = 1.0 \times 10^{12}$ M$_\odot$. We also reject at the 99 per cent confidence level a mass lower than $M_{125} = 5.4 \times 10^{11}$ M$_\odot$. The most likely orbit in this model galaxy potential is shown as a full line in the projections displayed in Figs 4 and 5 and its circular velocity curve is displayed in the same way in Fig. 6. This orbit manages to fit the distance information in fields 1–7 very well, but it is peculiar in being exceedingly radial (pericentre to apocentre ratio of 70). Indeed, the orbit has a tangential velocity in field 1, relative to M31, of 5 km s^{-1}, that is, the orbit has only a very small non-radial velocity component. This may be partly responsible for the good agreement of the present mass estimate with those estimates derived above for the three toy models in which radial orbits were imposed. In the present analysis we have again assumed that the tangential motion of M31 is negligible. However, the effect of a 300 km s^{-1} tangential velocity along the direction of the stream alters the derived mass inside 125 kpc by only 0.5×10^{11} M$_\odot$.

If we decide to also fit the distance data in fields 12 and 13, the most likely model has a much higher total mass inside 125 kpc, with

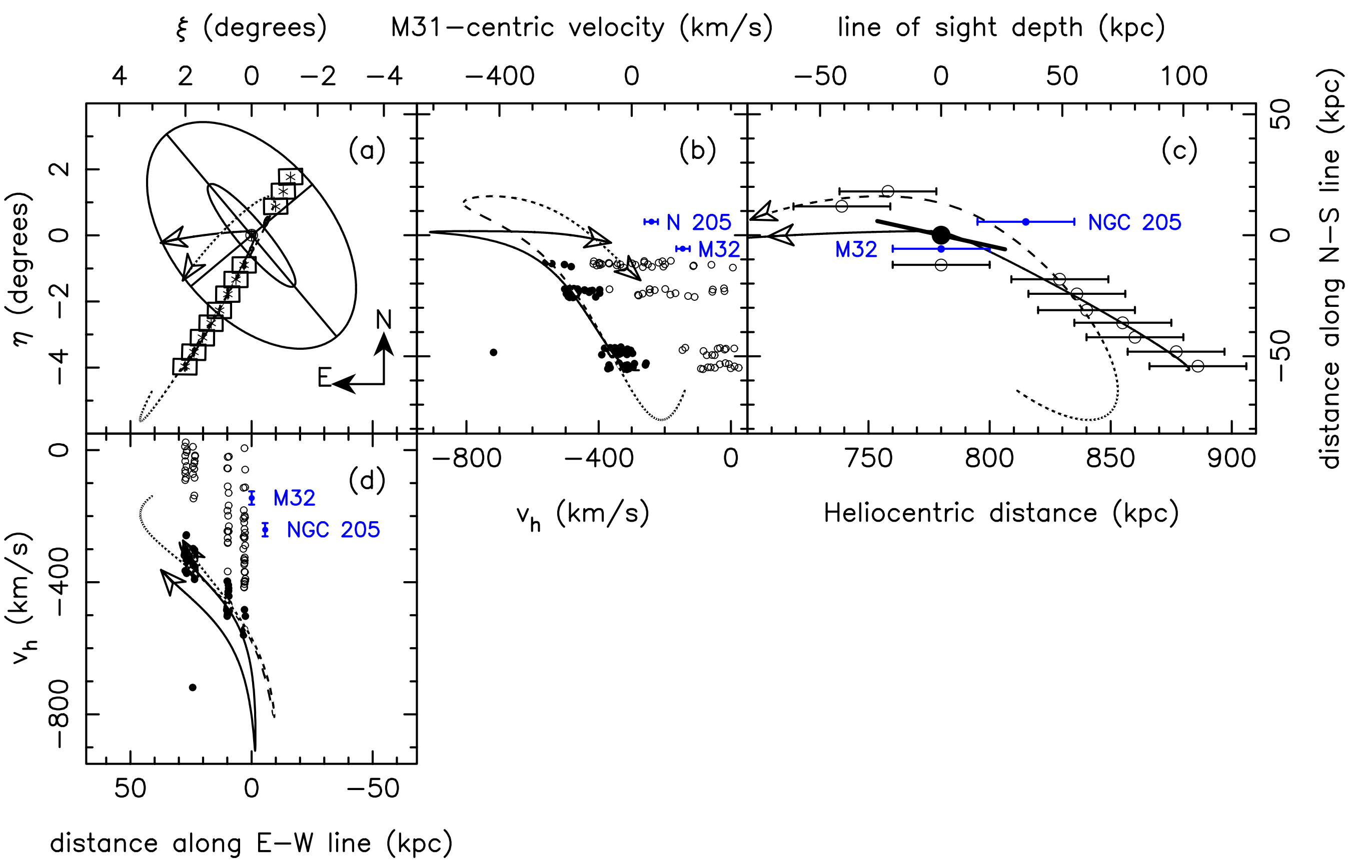

Figure 4. A multidimensional view of the two best-fitting orbits in the more realistic galaxy model of Klypin et al. (2002). The kinematics in Fig. 1, combined with the distance information of Fig. 2, require that the stream orbit is currently moving in towards M31, gaining velocity from field 1 to 6 as the stream approaches M31. The full line shows the orbit projection on the sky for the best-fitting orbit, in the best-fitting potential, when only the data in fields 1–8 are taken into account: in this case the total mass of M31 inside 125 kpc is $M_{125} = 7.5^{+2.5}_{-1.3} \times 10^{11}$ M$_\odot$. The dashed line however, shows the best-fitting orbit in the best-fitting potential when we also account for the distance data in fields 12 and 13. Now the mass of the model is $M_{125} = 1.5 \pm 0.1 \times 10^{12}$ M$_\odot$ inside 125 kpc. In both cases the curves display the centre-of-mass orbits, integrated for $\pm$ 0.75 Gyr from the position of the centre of field 6; the arrowheads show the direction of motion. Panel (a) shows the location on the sky of the two orbits superimposed on the chart previously shown in Fig. 1; panels (b) and (d) present projections of the distance–velocity relation (symbols as in Fig. 1); and finally panel (c) shows a sideways view of the orbits (as in Fig. 2).

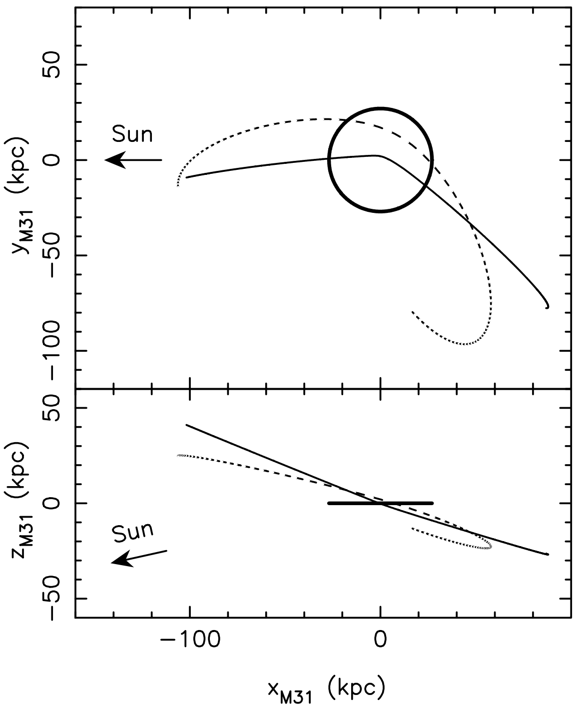

Figure 5. The paths, in M31-centric coordinates, of the two best-fitting orbits previously shown in Fig. 4. In this coordinate system, the Sun is located at $(x_{M31}, y_{M31}, z_{M31}) = (-762, 0, -169)$ kpc. The upper panel shows a face-on view of M31 (the limits of a 27 kpc radius disc is indicted with a thick circle), while the lower panel is an edge-on view of the plane of M31.

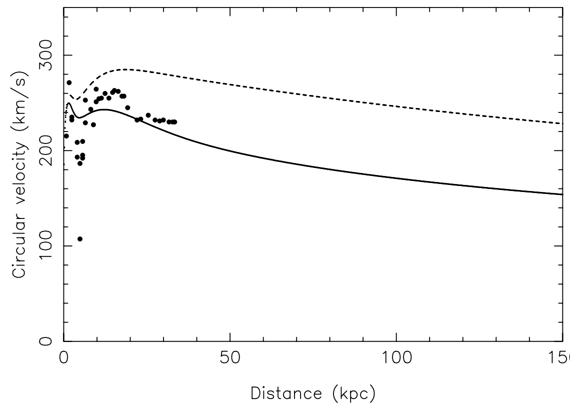

Figure 6. The circular velocity curve of the two best-fitting potentials. The high-mass model (dashed line), based on the assumption that the stream continues to fields 12 and 13, greatly over-predicts the observed rotation curve between 20–30 kpc. The M31 rotation curve data are reproduced here with solid dots (from the compilation by Klypin et al. 2002).

$M_{125} = 1.5 \pm 0.1 \pm 0.25 \times 10^{12}$ M$_\odot$ (again, the second uncertainty value reflects a tangential motion of M31 of 300 km s^{-1}). The most likely orbit in this potential model is shown with a dashed line in Figs 4 and 5, and the circular velocity of the potential is shown with a dashed line in Fig. 6. This orbit does not manage to fit the large line-of-sight distances in fields 1 and 2 as well as the previous case (although the discrepancy is not statistically significant given the large error bars on these distance data). The main shortcoming is that the circular velocity of this model at galactocentric distances below 30 kpc is at odds with the data displayed in Fig. 6. The circular velocity of the halo alone (without the bulge and disc) is higher than the data allow. This model is therefore not acceptable.

4 DISCUSSION AND CONCLUSIONS

In this first kinematic study of the giant stellar stream in the Andromeda galaxy, we have been able to measure the radial velocity gradient along the stream from the outermost field currently probed, 125 kpc distant from the centre of M31, down to an inner field ~ 20 kpc from the centre of that galaxy. Over this huge distance, the (projected) radial velocity changes by 245 km s^{-1}, implying a de-projected velocity difference of ~ 280 km s^{-1}. This velocity gradient is used to obtain a zeroth-order analytic estimate of the mass of the halo, which for simple halo-only galaxy models such as a logarithmic halo or an NFW halo, implies a mass inside 125 kpc of $M_{125} = 7.6 \pm 1.2 \times 10^{11}$ M$_\odot$ and $M_{125} = 6.4 \pm 1.3 \times 10^{11}$ M$_\odot$, respectively. In both cases, the uncertainty associated with a possible tangential velocity of M31 of 300 km s^{-1} is ~5 per cent.

We also investigate more realistic solutions, allowing the stream to have a non-radial orbit and taking a galaxy model that is the sum of a disc, bulge and dark halo (Klypin et al. 2002). The dark halo of this model is a perturbation on a spherical NFW model, to account for the adiabatic contraction of the dark matter as the baryonic components form. If we disregard the distance data in fields 12 and 13, because we cannot be certain that the stream is present in those regions, the most likely mass of this galaxy model is $M_{125} = 7.5^{+2.5}_{-1.3} \times 10^{11}$ M$_\odot$, with a lower limit of $M_{125} = 5.4 \times 10^{11}$ M$_\odot$ (at 99 per cent confidence). This result is fully consistent with the zeroth-order analytic estimates discussed above and suggests that the derived mass is not very sensitive to the adopted mass model. Furthermore, there is a reasonable agreement of the resulting rotation curve with the kinematics of previously observed disc tracers (see Fig. 6), despite the fact that the model was only fit to the kinematics of the stream. This agreement is the result, in part, of the fact that we have taken previously fitted models for the disc and bulge, but the halo contribution to the total rotation curve dominates beyond ~ 20 kpc and it is at these large distances that we have fitted the model to the stream data. This confers further confidence on the derived mass model. The uncertainty on the mass estimate as a result of the possible tangential velocity of M31 is likely not very large, approximately 7 per cent for a tangential velocity of 300 km s^{-1}. One of the main uncertainties in the present analysis is the flattening of the halo, which we have not explored, as the current data set does not provide sufficient constraints. Future studies, fitting *N*-body simulations to a larger kinematic sample of stream stars, can be expected to improve the mass estimate and also constrain the halo shape.

It is only recently that measurements of the mass of M31 beyond the edge of its gaseous disc have been possible. Courteau & van den Bergh (1999) analysed the velocities of seven Andromeda satellites, finding a total mass of $13.3 \pm 1.8 \times 10^{11}$ M$_\odot$. In contrast, using a larger sample of 10 satellite galaxies, 17 globular clusters and 9 planetary nebulae as test particles, Evans & Wilkinson (2000) found that the most likely total mass of M31 is $12.3^{+18}_{-6} \times 10^{11}$ M$_\odot$, approximately half of their Milky Way estimate of $19^{+36}_{-17} \times 10^{11}$ M$_\odot$. With improved radial velocities of the M31 satellites they were later able to reduce their M31 mass uncertainties, finding a value of the total mass of $\sim 7.0^{+10.5}_{-3.5} \times 10^{11}$ M$_\odot$ (Evans et al. 2000), which is fully consistent with our result of $M_{125} = 7.5^{+2.5}_{-1.3} \times 10^{11}$ M$_\odot$ (defined within a radius of 125 kpc). However, a definitive statement of the relative masses of M31 and the Milky Way awaits an improved measurement for the Milky Way.

The best-fitting orbit in the best-fitting potential is prograde and, in the region where it is currently observed, it lies close to the plane of M31. Thus, it appears that the orbit of the Andromeda stream is peculiar in being extremely radial, passing very close (within 2 kpc) of the centre of M31. This requires very special initial conditions. The stream stars, which are spatially narrowly confined in fields 1 to 8, will diverge dramatically upon passing close to M31 to form a low-density fan-like structure, because orbits that deviate only slightly from the orbit displayed in Fig. 4 on the plunging part of their course will take very different paths after being accelerated around the centre of M31, as demonstrated in Fig. 7. The fanning out of the stream is likely to confuse efforts to measure the metallicity and age of the M31 halo: for instance, the recent discovery by Brown et al. (2003) of a young halo component in M31 from main-sequence fitting of an extremely deep Advanced Camera for Surveys (ACS) field may be the result of stream contamination (see Fig. 7).

Thus, the stream may be in the process of vanishing as a coherent structure, providing a supply of metal-rich stars into the halo. This also suggests that the stream was removed from its progenitor less than an orbital period ago (the pericentre-to-pericentre period of the continuous-line orbit in Fig. 4 is 1.8 Gyr), as we would otherwise not observe the structure as a stream. The ephemeral nature of the stream implies that the progenitor must have survived until ∼1.8 Gyr ago. As we discuss further below, the progenitor was probably of low mass, implying that the rate of decay of its orbit as a result of dynamical friction was slow, so it followed (or continues to follow) an orbit close to the current orbit of the stream. However, any dwarf galaxy on the derived orbit must have experienced extreme tides as it repeatedly passed close to the centre of M31. One option is that the progenitor was a very dense dwarf galaxy that was sufficiently robust to survive the huge tides. This brings to mind M32 as a candidate, though detailed numerical modelling is required to examine this possibility. The alternative option is that the progenitor of the stream deflected off another halo object, sending it plunging into the current orbit, analogous to the suggestion by Zhao (1998) to explain the longevity of the Galactic satellite Sagittarius.

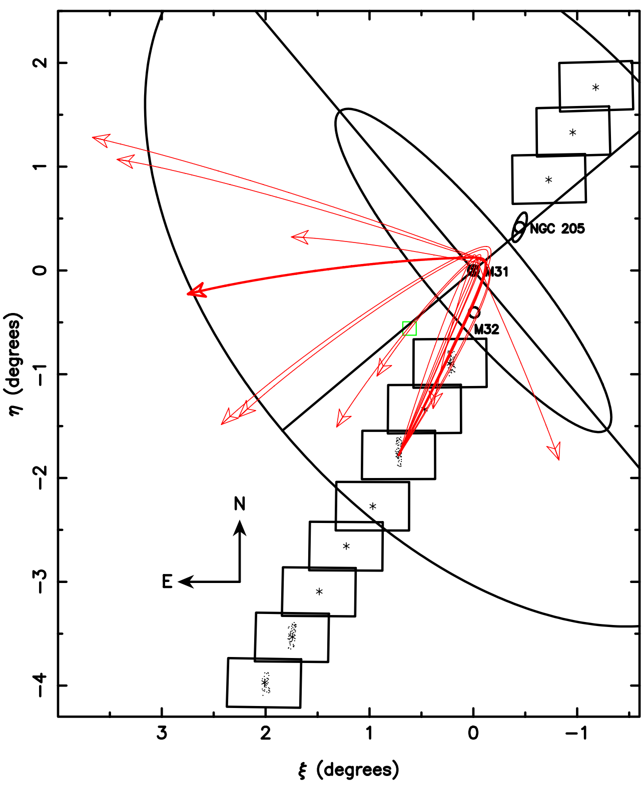

Figure 7. The spreading of orbits after a close encounter with M31. The thick line orbit reproduces the best-fitting orbit in the realistic galaxy potential previously shown in Fig. 4, integrated from the centre of field 6. The thin lines show similar orbits, starting from the same spatial position, but with velocities perturbed by a random offset drawn from a Gaussian distribution of dispersion 11 km s^{-1}. This fanning-out of stars on nearby orbits will lead to the disappearance of the Andromeda stream and implies that it is a transient phenomenon. The small square on the minor axis shows the position of the Brown et al. (2003) ACS field (not drawn to scale). All other markings are as in Fig. 1.

However, the connection with M32 presents some difficulties. Although M32 appears to reside in the stream, its velocity is markedly different. For M32 to be associated with the stream would require it to be at a different phase in the orbit (either lagging or trailing). Furthermore, the low-velocity dispersion of the stream would appear to preclude M32 as its progenitor (which has $\sigma_v \sim 50$ km s^{-1} outside the nucleus: van der Marel et al. 1994), though this cannot be confirmed without a detailed dynamical study. The case for association of NGC 205 with the stream also appears weaker given these kinematic measurements, because the best-fitting orbit does not overlap with it in phase space. Future studies may allow us to examine this issue in more detail by following the stream beyond the region currently probed with kinematics. The velocities of the stream stars presented here also shed light on the recent identification of a possible new companion to M31, And VIII (Morrison et al. 2003). The radial velocities of those planetary nebulae, which are located close to M32 (see Fig. 1), appear to have radial velocities consistent with an extrapolation of the stream, as they lie close to the straight line in the right-hand panel of Fig. 1. This would suggest that And VIII is most likely part of the Andromeda stream, situated in the region of highest over-density reported by Ibata et al. (2001b). However, it is interesting to note that the radial velocities of the Morrison et al. (2003) planetary nebula sample tend to increase towards the north (showing an apparent positive gradient in the right-hand panel of Fig. 1), whereas the stream stars have a negative velocity gradient. The connection between the two structures therefore merits more careful examination. During the refereeing process, a study by Merrett et al. (2003) was presented, which also investigates the planetary nebulae around M31. However, though their survey has also detected planetary nebulae in a region at the base of the stream (near our field 8), their interpretation is inconsistent with the kinematics of the stars reported here. The direction of motion of the orbit they derive is opposite to ours and the path of their orbit, which intercepts many M31-disc PNe, is substantially different to the orbit that we have fitted. It is possible that their finding reveals the presence of another kinematic structure in Andromeda.

The majority of the stream stars that were surveyed have a narrow velocity dispersion of 11 ± 3 km s^{-1}, though slightly skewed to positive velocities. The fact that our line of sight looks down the stream (see Fig. 2), so that we probably see stars over a range of distance along the line of sight and hence at different phases in the orbit, will tend to render the observed velocity dispersion higher than the intrinsic velocity dispersion. This indicates that the progenitor was most likely a low-mass dwarf galaxy. The Milky Way satellite Sagittarius, which has a velocity dispersion of 11 km s^{-1} (Ibata et al. 1997), also has a gigantic stellar stream, but with a larger velocity dispersion of 20 km s^{-1} (Yanny et al. 2003). However, it is unclear at present whether the lower velocity dispersion measured in the

Andromeda stream compared with the Sagittarius stream implies that its progenitor was of lower mass than Sagittarius, or not.

ACKNOWLEDGMENTS

RI would like to thank A. Klypin and H.-S. Zhao for kindly providing their compilation of M31 disc kinematics and for explaining the details of their Andromeda galaxy model. The anonymous referee is thanked for comments that improved the paper. The research of AMNF has been supported by a Marie Curie Fellowship of the European Community under contract number HPMF-CT-2002-01758.

REFERENCES

Brown T. et al., 2003, ApJ, 592, L17
Bullock J., Kolatt T., Sigad Y., Somerville R., Kravtsov A., Klypin A., Primack J., Dekel A., 2001, MNRAS, 321, 559
Courteau S., van den Bergh S., 1999, AJ, 118, 337
Dehnen W., Binney J., 1998, MNRAS, 294, 429
de Vaucouleurs G., de Vaucouleurs A., Corwin H., Buta R., Paturel G., Fouque P., 1991, Third Reference Catalogue of Bright Galaxies. Springer-Verlag, Berlin
Einasto J., Lynden-Bell D., 1982, MNRAS, 199, 67
Evans N., Wilkinson M., 2000, MNRAS, 316, 929
Evans N., Wilkinson M., Guhathakurta P., Grebel E., Vogt S., 2000, ApJ, 540, L9
Ferguson A., Irwin M., Ibata R., Lewis G., Tanvir N., 2002, AJ, 124, 1452
Gould A., 1994, ApJ, 435, 573
Helmi A., White S., 1999, MNRAS, 307, 495
Ibata R., Wyse R., Gilmore G., Irwin M., Suntzeff N., 1997, AJ, 113, 634
Ibata R., Lewis G., Irwin M., Totten E., Quinn T., 2001a, ApJ, 551, 294
Ibata R., Irwin M., Lewis G., Ferguson A., Tanvir N., 2001b, Nat, 412, 49
Ibata R., Lewis G., Irwin M., Cambrésy L., 2002, MNRAS, 332, 921
Johnston K., Zhao H.-S., Spergel D., Hernquist L., 1999, ApJ, 512, L109
Johnston K., Sackett P., Bullock J., 2001, ApJ, 557, 137
Kahn F., Woltjer L., 1959, ApJ, 130, 705
Klypin A., Zhao H.-S., Somerville R., 2002, ApJ, 573, 597
Lynden-Bell D., Lin D., 1977, MNRAS, 181, 37
Majewski S., Skrutskie M., Weinberg M., Ostheimer J., 2003, ApJ, 599, 1082
Malin D., Hadley B., 1997, Publ. Astron. Soc. Aust., 14, 52
McConnachie A., Irwin M., Ibata R., Ferguson A., Lewis G., Tanvir N., 2003, MNRAS, 343, 1335
Merrett H. et al., 2003, MNRAS, 346, 62
Morrison H., Harding P., Hurley-Keller D., Jacoby G., 2003, ApJ, 596, L183
Navarro J., Frenk C., White S., 1997, ApJ, 490, 493
Pohlen M., Martinez-Delgado D., Majewski S., Palma C., Prada F., Balcells M., 2003, in Prada F., Martinez-Delgado D., Mahoney T., eds, ASP Conf. Ser., Satellites and Tidal Streams. Astron. Soc. Pac., San Francisco, in press (astro-ph/0308142)
Press W., Flannery B., Teukolsky S., Vetterling W., 1992, Numerical Recipes. Cambridge Univ. Press, Cambridge
Reitzel D., Guhathakurta P., 2002, AJ, 124, 234
Stanek K., Garnavich P., 1998, ApJ, 503, L131
van der Marel R., Rix H.-W., Carter D., Franx M., White S., de Zeeuw T., 1994, MNRAS, 268, 521
Yanny B. et al., 2003, ApJ, 588, 824
Zhao H.-S., 1998, ApJ, 500, L149
Zhao H.-S., Johnston K., Henquist L., Spergel D., 1999, A&A, 348, 49

This paper has been typeset from a TEX/LATEX file prepared by the author.